Neuro-Oncology Practice
11(2), 142–149, 2024 | https://doi.org/10.1093/nop/npad081 | Advance Access date 5 January 2024

RT-PCR assay to detect *FGFR3::TACC3* fusions in formalin-fixed, paraffin-embedded glioblastoma samples

Loudy P. Priesterbach-Ackley, Joyce van Kuik, Bastiaan B.J. Tops, Anna Lasorella, Antonio Iavarone, Wim van Hecke, Pierre A. Robe, Pieter Wesseling, and Wendy W.J. de Leng

All author affiliations are listed at the end of the article

Corresponding Author: Loudy P. Priesterbach-Ackley, MD, MSc, Department of Pathology, University Medical Center Utrecht, Heidelberglaan 100, 3584 CX Utrecht, The Netherlands (L.P.Priesterbach-3@umcutrecht.nl).

Abstract

Background. One targeted treatment option for isocitrate dehydrogenase (*IDH*)-wild-type glioblastoma focuses on tumors with fibroblast growth factor receptor 3::transforming acidic coiled-coil-containing protein 3 (*FGFR3::TACC3*) fusions. *FGFR3::TACC3* fusion detection can be challenging, as targeted RNA next-generation sequencing (NGS) is not routinely performed, and immunohistochemistry is an imperfect surrogate marker. Fusion status can be determined using reverse transcription polymerase chain reaction (RT-PCR) on fresh frozen (FF) material, but sometimes only formalin-fixed, paraffin-embedded (FFPE) tissue is available.

Aim. To develop an RT-PCR assay to determine *FGFR3::TACC3* status in FFPE glioblastoma samples.

Methods. Twelve tissue microarrays with 353 historical glioblastoma samples were immunohistochemically stained for FGFR3. Samples with overexpression of FGFR3 ($n = 13$) were subjected to *FGFR3::TACC3* RT-PCR on FFPE, using 5 primer sets for the detection of 5 common fusion variants. Fusion-negative samples were additionally analyzed with NGS ($n = 6$), FGFR3 Fluorescence In Situ Hybridization ($n = 6$), and RNA sequencing ($n = 5$).

Results. Using RT-PCR on FFPE material of the 13 samples with FGFR3 overexpression, we detected an *FGFR3::TACC3* fusion in 7 samples, covering 3 different fusion variants. For 5 of these FF was available, and the presence of the fusion was confirmed through RT-PCR on FF. With RNA sequencing, 1 additional sample was found to harbor an *FGFR3::TACC3* fusion (variant not covered by current RT-PCR for FFPE). The frequency of *FGFR3::TACC3* fusion in this cohort was 9/353 (2.5%).

Conclusions. RT-PCR for *FGFR3::TACC3* fusions can successfully be performed on FFPE material, with a specificity of 100% and (due to limited primer sets) a sensitivity of 83.3%. This assay allows for the identification of potential targeted treatment options when only formalin-fixed tissue is available.

Keywords

FFPE | FGFR3::TACC3 fusion | glioblastoma | RT-PCR

Successful (targeted) therapy options for isocitrate dehydrogenase (*IDH*)-wild-type glioblastoma (GBM) are greatly desired.[1] Rapid advances in tumor genotyping are creating opportunities for the identification of targeted treatments from which at least a subset of patients might benefit. One such approach focuses on targeting gene fusions involving fibroblast growth factor receptor 3 (*FGFR3*) and the coiled-coil domain of the transforming acidic coiled-coil-containing protein 3 (*TACC3*). This is the most prevalent identified gene fusion in adult gliomas, occurring in 3.0%–8.3% of *IDH*-wild-type gliomas.[2–5] *FGFR3::TACC3* fusion occurs mostly in *IDH*-wild-type GBM,[6] including in histologically lower-grade *IDH*-wild-type diffuse astrocytomas with molecular features of GBM.[7] Interestingly, a better survival rate has been reported for GBM cases positive for *FGFR3::TACC3* fusion compared to cases without this fusion.[6,8,9]

The biology of FGFR::TACC fusion proteins is not completely understood,[10] but it is hypothesized that the *FGFR3* fusion

leads to loss of the microRNA (miR)-99a binding site, resulting in FGFR3 overexpression.[11] The oncogenic effects may then be caused by accumulation of the proteins in the nucleus and direct phosphorylation of substrates that are essential for mitosis while concurrent activation of growth-promoting pathways allows the cells to remain viable.[12] More recently, it was suggested that the *FGFR3::TACC3* fusion is oncogenic due to the activation of oxidative phosphorylation and mitochondrial metabolism.[13] In addition, FGFR3::TACC3 fusion protein might be able to induce mitotic segregation defects leading to aneuploidy, when localized at the mitotic spindle poles.[5,14]

Two phase I trials of Erdafitinib (JNJ-42756493), an oral pan-FGFR inhibitor, have independently shown the response of 3 patients ($n = 2$ in 1 trial, $n = 1$ in the other trial) with *FGFR3::TACC3* fusion-positive GBM.[2,13,15] Wang et al. described 1 case in which a patient with *FGFR3::TACC3* fusion-positive, *TERT* promoter mutant GBM was treated with Anlotinib (multi-target tyrosine kinase inhibitor) and temozolomide, resulting in a partial response that was maintained for more than 17 months.[16] There are several ongoing trials that include patients with glioblastoma, *IDH*-wild-type, to test treatment targeting FGFR-signaling (not all limited to FGFR fusion-positive tumors).[17]

It is essential to carefully select patients who are eligible for targeted treatments.[6,9] Thus, it is important to identify *FGFR3::TACC3* fusions in a specific and sensitive manner. However, the detection can be challenging because of the structural heterogeneity of the *FGFR3::TACC3* fusions, with 15 distinct breakpoints described.[18] Ideally, fusion detection should be performed using RNA-based techniques, to confirm whether the case meets the genomic criteria for trial inclusion.

Although it has been suggested that *FGFR3::TACC3* fusion-positive GBM cases can have a specific morphology (tumor cells with monomorphous ovoid nuclei, nuclear palisading, a fine network of capillary vessels, microcalcifications, and desmoplasia[19]), a recent case series showed that morphology alone is not reliable for identification of cases that are suspect for *FGFR3::TACC3* fusion.[20] For screening purposes, it is possible to stain accumulated FGFR3::TACC3 proteins through immunohistochemistry (IHC) with an antibody against the N-terminal of FGFR3.[12] In normal brain tissue or glioma without *FGFR3* aberration, this staining should be negative due to the suppression of FGFR3 protein expression by miRNA 99a.[4] Staining for FGFR3 can be diffuse cytoplasmic, sometimes nuclear and/or membranous.[11] The sensitivity of FGFR3 IHC to detect *FGFR3::TACC3* fusion was reported to be 100% and the specificity 88% for samples with moderate-to-strong staining intensity.[11]

Several options are available to test for the presence of *FGFR3::TACC3* fusions. A real-time (reverse transcription) polymerase chain reaction (RT-PCR) assay has been developed previously to detect all *FGFR3::TACC3* variants using a single primer set,[2] but this can only be used for fresh frozen (FF) samples. Targeted RNA sequencing would be useable in this context; however, many labs do not have access to this technique. Next-generation sequencing (NGS) is not suitable for *FGFR3::TACC3* fusion detection, as targeted DNA NGS panels that are used for mutation detection do not cover intronic regions to detect the breakpoints and the change in coverage caused by the duplication is too small to allow for reliable detection. Fluorescence In Situ Hybridization (FISH) is a technique that can be performed on FFPE material for fusion detection, but this is not suitable for the detection of *FGFR3::TACC3* fusion due to the close proximity of *FGFR3* and *TACC3* on chromosome 4.[2]

While formalin-fixation and paraffin embedding (FFPE) is the most commonly used manner of tissue preservation in pathology, many molecular techniques perform suboptimal on FFPE samples. This is mainly due to DNA fragmentation. This fragmentation occurs significantly less in FF material, which is why FF samples are preferred for many molecular techniques. However, FF samples are often not available. In this study, we examine the sensitivity and specificity of an RT-PCR assay designed to detect 5 *FGFR3::TACC3* fusion variants in FFPE GBM samples. The present study was designed to investigate the feasibility of RT-PCR as a tool for *FGFR3::TACC3* fusion detection in FFPE samples.

Materials and Methods

Tissue Samples

In this study, we analyzed 12 tissue microarrays (TMAs; University Medical Center, Utrecht) with a total of 353 historical glioblastoma samples, constructed from FFPE tissue blocks. The samples dated from 2005 to 2014. IDH1 immunohistochemical staining was performed on the TMA's: 94.2% of samples were negative for IDH1 staining. *IDH* mutation analysis was not routinely investigated; therefore, *IDH1* mutation status was not confirmed at DNA level and *IDH2* mutation status of the samples is unknown. It is estimated that >94% of samples would now be diagnosed as "glioblastoma, *IDH*-wildtype" and a few cases as "high-grade astrocytoma, *IDH*-mutant" using the current diagnostic criteria. However, this should not impede the aim of the study. The TMAs contained 3 cores (0.6 mm) from different areas of each tumor. Snap-frozen samples were collected with informed consent of the patients (METC 09-420 and 16-342).

FGFR3 N-Terminus Immunohistochemistry

TMA slides (4 µm) were stained with a mouse monoclonal antibody raised against the N-terminal region of FGFR3 (specifically against amino acids 15-124 of FGFR3 of human origin, SC-13121, Santa Cruz Biotechnology, Dallas, TX; dilution 1:200), using the Ventana Benchmark Ultra automated staining instrument (Ventana Medical Systems, Tucson, AZ), according to manufacturer instructions. Expression of FGFR3 was semiquantitatively scored by 1 neuropathologist (W.H.), based on staining intensity: 0 (negative, N), 1+ (low, L), 2+ (high, H), as described previously by Theelen et al.[21] The highest score of the 3 TMA tissue cores from each sample was used to select cases for further analysis, to compensate for intratumoral heterogeneity. Of the samples that showed at least 1 TMA core with positive FGFR3 staining, corresponding whole-tumor FFPE slides were stained as well.

RNA Extraction and cDNA Synthesis

Total RNA was extracted from FF tissue using RNeasy Mini Kit (Qiagen, Hilden, Germany) and from FFPE tissue using RNeasy FFPE kit (Qiagen, Hilden, Germany) according to manufacturer instructions. For 2 samples (samples 7 [FFPE] and 14 [FFPE], analyzed at a later point in time), RNA was isolated using Maxwell RSC automated instrument according to manufacturer instructions. One to three micrograms of total RNA were retrotranscribed using Superscript III (Invitrogen), Oligo-dT15 (Promega), and Random primers (Promega) according to respective manufacturers' instructions.

RT-PCR on FF

RT-PCR of *FGFR3::TACC3* was performed on FF material by applying the protocol from Lasorella et al.[12] The PCR mix consisted of 2.5 µL PCR buffer, 1 µL dNTP (10 mM), 0.75 µL forward primer, 0.75 µL reverse primer (0.3 uM), 0.5 µL $MgSO_4$ (50 mM), 0.2 µL platinum Taq DNA polymerase (Thermo Fisher Scientific), 1 µL (50 ng) complementary DNA (cDNA), and up to 25 µL Milli-Q. The primers used for FF were *FGFR3*exon11-Forward: 5'-CGTGAAGA TGCTGAAAGACGATG-3' and *TACC3*exon14-Reverse: 5'-AAACGCTTGAAGAGGTCGGAG-3'. Amplification conditions were: 94°C for 3 minutes, 40 cycles "94°C—30 seconds, 58°C—30 seconds, 68°C—1 minute 40 seconds" and finally 68°C for 7 minutes. The RT-PCR assay was first tested on GBM-1123, a case known to be positive for the *FGFR3::TACC3* fusion.[5] Subsequently, GBM-1123 was used as a positive control.

RT-PCR on FFPE

The PCR protocol and reagents used for FFPE material were the same as for FF material. Except, instead of 1 µL cDNA, 10 µL cDNA was used as input for the PCR reaction, and different primers were used.

For FFPE samples, 5 primer sets were created for 5 of the most commonly observed fusion variants (Supplementary Table 2), covering 60% of previously reported *FGFR3::TACC3* fusions in human gliomas.[18] These covered the fusion variants: *FGFR3*ex17::*TACC3*ex11 (20%), 17-8 (14%), 17-10 (11%), 17-6 (9%), 18-5 (6%). Forward primers were created for *FGFR3* and reverse primers were created to be reverse complimentary to different regions in the *TACC3* gene. The PCR program was the same as for FF. The quality of the cDNA from FFPE tissue was verified through the presence of the reference genes *GAPDH* (100 base pairs [bp] amplified product) and β-*actin* (274 bp amplified product).

Synthetic DNA sequences were used as a positive control to compare *FGFR3::TACC3* positive FFPE samples to the predicted amplicon lengths (Figure 1). After amplification by fusion-specific PCR, agarose gel electrophoresis was performed to confirm the presence of the product based on the expected length of the amplicon. Next, the PCR products were purified and subjected to Sanger sequencing. BLAST analysis was performed using *FGFR3* (NM_000142) and *TACC3* (NM_006342) reference sequences.

Fluorescence In Situ Hybridization

FGFR3 IHC positive, but *FGFR3::TACC3* fusion-negative samples were analyzed with FISH for potential *FGFR3* amplification. FFPE slides were hybridized with an *IGH/FGFR3* (*IGH*, immunoglobulin heavy locus) translocation dual fusion FISH probe (Cytocell, Cambridge, UK). FFPE slides were prepared for FISH using protocol as described by Richardson et al.[22] To determine *FGFR3* gene copy numbers, 50 tumor cell nuclei per tumor were assessed on *FGFR3* and *IGH* gene copy numbers at 100× magnification using a Leica DM5500 B microscope system with Leica application suite advanced fluorescence software (Leica Microsystems, Rijswijk, The Netherlands). An *FGFR3-IGH* ratio was calculated and defined as

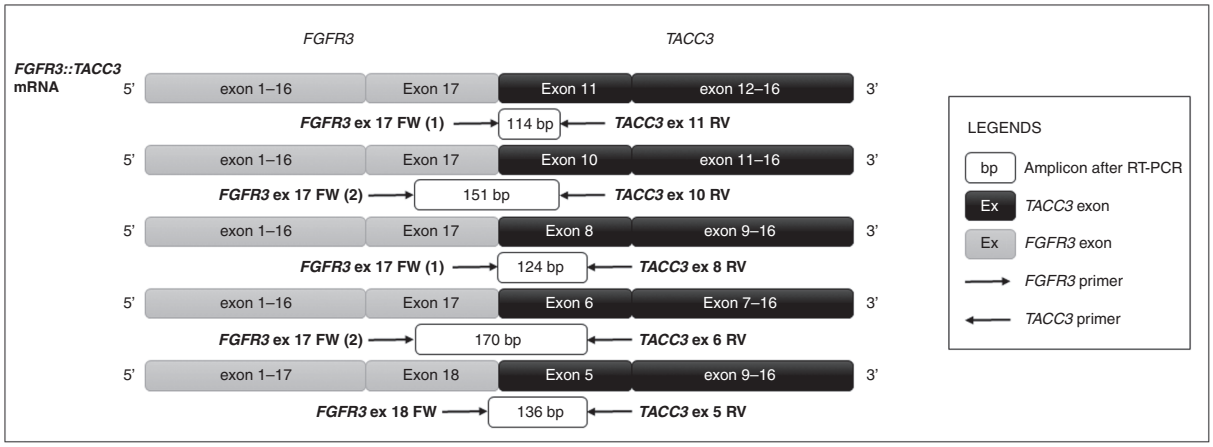

Figure 1. Schematic representation of the primers used in the RT-PCR assay for FFPE material and the expected amplicon length of the product in base pairs (bp). For the exact sequences and references, see Supplementary Table 2.

<1.5: normal copy numbers, 1.5–2.0: copy number gain, >2: gene amplification.[23]

Next-Generation Sequencing

FGFR3 IHC positive, but *FGFR3::TACC3* fusion-negative samples were also analyzed with NGS[24] to detect a possible mutation in *FGFR3*. The panel includes *FGFR3* codon 248–277, 368–402, 632–653, 691–719, and 772-807. Other mutations/amplifications found were also reported (Supplementary Table 1).

RNA Sequencing

Total RNA was isolated from FF samples using Maxwell RSC automated instrument according to manufacturer instructions, aiming for a minimum concentration of 20 ng/µL. Library preparation, sequencing, and data analysis were performed as described in the article by J. Hehir-Kwa et al.[25] In short, RNAseq libraries were generated with 300 ng RNA using the KAPA RNA HyperPrep Kit with RiboErase (Roche) and subsequently sequenced on a NovaSeq 6000 system (2 × 150 bp) (Illumina). The RNA sequencing data were processed as per the GATK 4.0 best practices workflow for variant calling, using a wdl- and cromwell-based workflow (https://gatk.broadinstitute.org/hc/enus/sections/360007226651-Best-Practices-Workflows). This included performing quality control with Fastqc (version 0.11.5) to calculate the number of sequencing reads and the insert size, Picard (version 2.20.1) for RNA metrics output and MarkDuplicates. The raw sequencing reads were aligned using Star (version 2.7.0f) to Genome Reference Consortium Human Build 38 and gencode version 29. Gene fusion detection was performed using Star fusion (version 1.6.0).[26]

Results

FGFR3 IHC Screening

TMA slides were screened for FGFR3 overexpression using FGFR3 IHC. Out of 353 samples, 308 were interpretable (with at least 1 evaluable tissue core) (Figure 2). Out of 308 glioblastoma samples, 13 samples (4.2%) showed low (1+, $n = 10$) or high (2+, $n = 3$) FGFR3 staining intensity (Table 1). An example of high- and low-intensity staining patterns is shown in Supplementary Figure 1. Expression of FGFR3 fusion protein was verified on whole FFPE tissue slides using the same N-terminal FGFR3 antibody. Of these, 4 showed homogeneous expression of the tumor tissue, whereas 9 showed intratumoral heterogeneity for FGFR3 staining with both positive and negative tumor areas. Both homogeneous and heterogeneous staining patterns varied in intensity. All cases positive for FGFR3 IHC on TMA were also positive on their corresponding whole slide, though in a few cases, staining intensity differed between TMA and whole slide, as exemplified in Table 1.

RT-PCR Assay for Detection of FGFR3::TACC3 Fusions on FF/FFPE

FGFR3::TACC3 RT-PCR was performed on the 13 FGFR3 IHC-positive samples to check for the presence of a fusion. Together, the RT-PCR assay on 13 FFPE samples

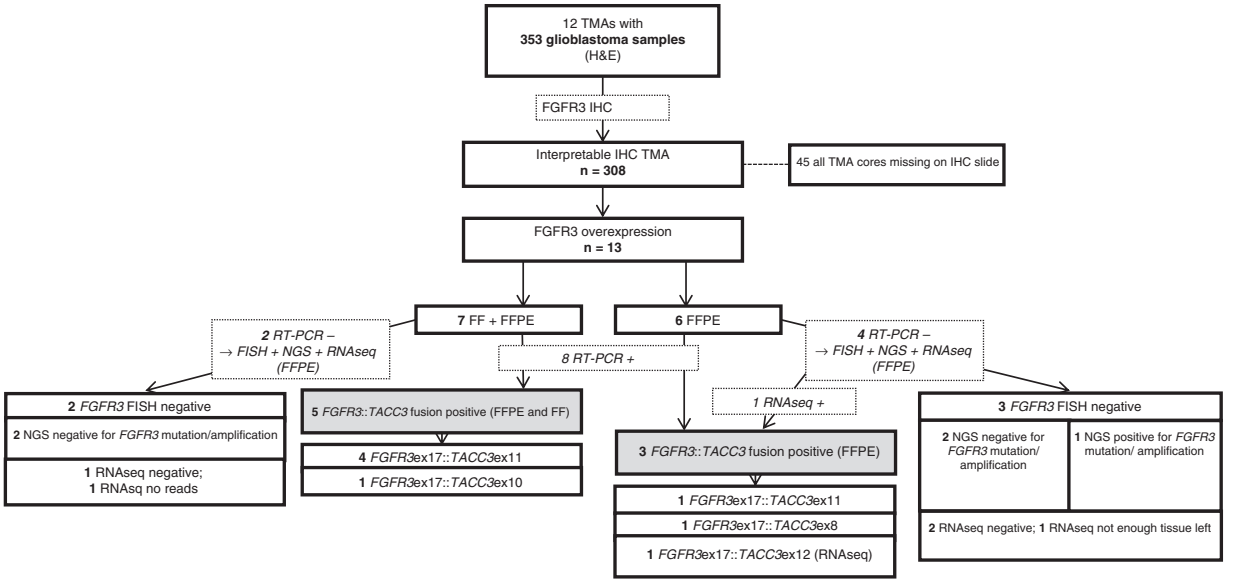

Figure 2: Flow diagram showing sample selection and results. The cohort consisted of 353 historical glioblastoma samples in 12 tissue microarrays (TMAs). FGFR3 IHC was interpretable for 308 samples, of which 13 showed FGFR3 overexpression (1+ or 2+). Out of these 13 samples, 7 were positive for *FGFR3::TACC3* fusion upon testing of FFPE material with RT-PCR. One additional sample with *FGFR3::TACC3* fusion was found with RNA sequencing. The remaining samples were all negative for *FGFR3* amplification (tested with fluorescence in situ hybridization [FISH]), and only 1 sample had an *FGFR3* mutation upon testing with next-generation sequencing.

Table 1: Overview of all 13 cases with positive IHC on TMAs

Case ID	Dx	FGFR3 IHCTMA	FGFR3 IHC whole slide	RT-PCR (FFPE)	RNAseq (FF)
1	GBM	1+	Heterogeneous, 1+	negative	No reads
2	GBM	1+	Heterogeneous, 1+	*FGFR3*ex17::*TACC3*ex10	—
3	GBM	1+	Heterogeneous, 1+	negative	negative
4	GBM	1+	Homogeneous, 2+	*FGFR3*ex17::*TACC3*ex11	—
5	GBM	2+	Homogeneous, 2+	*FGFR3*ex17::*TACC3*ex11	—
6	GBM	2+	Heterogeneous, 2+	*FGFR3*ex17::*TACC3*ex11	—
7	GBM	1+	Homogeneous, 2+	*FGFR3*ex17::*TACC3*ex8	—
8	GBM	2+	Homogeneous, 2+	*FGFR3*ex17::*TACC3*ex11	—
9	GBM	1+	Heterogeneous, 2+	*FGFR3*ex17::*TACC3*ex11	—
10	GBM	1+	Heterogeneous, 1+	negative	N/A
11	GBM	1+	Heterogeneous, 2+	negative	*FGFR*ex17::*TACC3*ex12
12	GBM	1+	Heterogeneous, 1+	negative	negative
13	GBM	1+	Heterogeneous (very focal), 1+	negative	negative

revealed 7 *FGFR3::TACC3* positive samples (Table 1) consisting of the 3 most commonly observed fusion variants: *FGFR3*ex17::*TACC3*ex11 ($n = 5$), *FGFR3*ex17::*TACC3*ex8 ($n = 1$), and *FGFR3*ex17::*TACC3*ex10 ($n = 1$). An example of each is shown in Figure 3. The PCR products including the breakpoints of the 3 fusion variants were validated by Sanger sequencing (Supplementary Figure 2). For 5 cases for which FF material was available, the presence of the fusion was confirmed using RT-PCR on FF tissue.

Additional Molecular Analyses to Explain FGFR3 Overexpression

To investigate the possible alternative explanations of FGFR3 overexpression in the 6 FGFR3 IHC positive but *FGFR3::TACC3* fusion-negative samples, FISH was performed to assess for *FGFR3* copy-number gain or *FGFR3* amplification. All 6 samples showed a normal ($n = 2$) *FGFR3* gene copy number. To check whether the FGFR3 overexpression in these samples could be explained by an activating point mutation in *FGFR3*, the samples were subjected to NGS using a Cancer Hotspot panel. In one of the 5 samples, an inactivating *FGFR3* mutation was detected: Case 13, *FGFR3* mutation p.(Asp785Argfs*31), which does not explain FGFR3 expression with IHC. The other genetic alterations that were detected through NGS are reported in Supplementary Table 1. Finally, RNA sequencing revealed 1 additional case with an *FGFR3::TACC3* fusion: Case 11 showed variant *FGFR3*ex17::*TACC3*ex12, which is not covered by the 5 primer sets we used in the RT-PCR assay for FFPE material.

Sensitivity, Specificity, and Predictive Value of RT-PCR on FFPE

Sensitivity, specificity, and predictive value could only be calculated for the limited number of cases for which both RT-PCR on FFPE and RT-PCR on FF or RNA sequencing were performed ($n = 9$). This analysis does not include 2 FGFR3 IHC-positive cases for which RNA sequencing was not successful and 2 fusion-positive cases upon RT-PCR on FFPE, for which no FF tissue was available.

Positive predictive value and negative predictive value for RT-PCR test on FFPE were both found to be 100%. Also, the specificity was 100%. As expected (because of the fact that the current RT-PCR method for FFPE does not cover all possible fusion variants), sensitivity was 83.3% (Supplementary Table 3).

Discussion and Conclusions

The occurrence of *FGFR* aberrations in GBM *IDH*-wild-type is relatively low: frequencies in the range of ~3% for *FGFR* rearrangements[5] to ~8% for all types of FGFR aberrations[27] are reported. *FGFR3* is most frequently altered in this context, but several types of tests would be needed to detect all possible changes involving *FGFR3* (i.e., mutations, amplifications, and translocations). Meanwhile, as FGFR3 accumulates at high levels in *FGFR3::TACC3* fusion-positive cases, positive FGFR3 immunostaining can be used for prescreening of cases that require further analysis to sort out the exact nature of the *FGFR3* alterations.

In this study, we showed that RT-PCR for the detection of *FGFR3::TACC3* fusions can successfully be performed on FFPE material, as well as on FF material. Out of 14 samples with FGFR3 overexpression on IHC, an *FGFR3::TACC3* fusion variant was detected using RT-PCR in 8 FFPE samples. For 5 of these, FF was available, and the result was confirmed using FF material. RNA sequencing revealed one more sample with an *FGFR3*ex17::*TACC3*ex12 fusion, which was not included in our RT-PCR assay. In 1 sample with FGFR3 overexpression but no *FGFR3::TACC3* fusion on RT-PCR and RNAseq, an inactivating *FGFR3* mutation was found. It was previously suggested that activating *FGFR3* mutations do not occur in diffuse gliomas due to

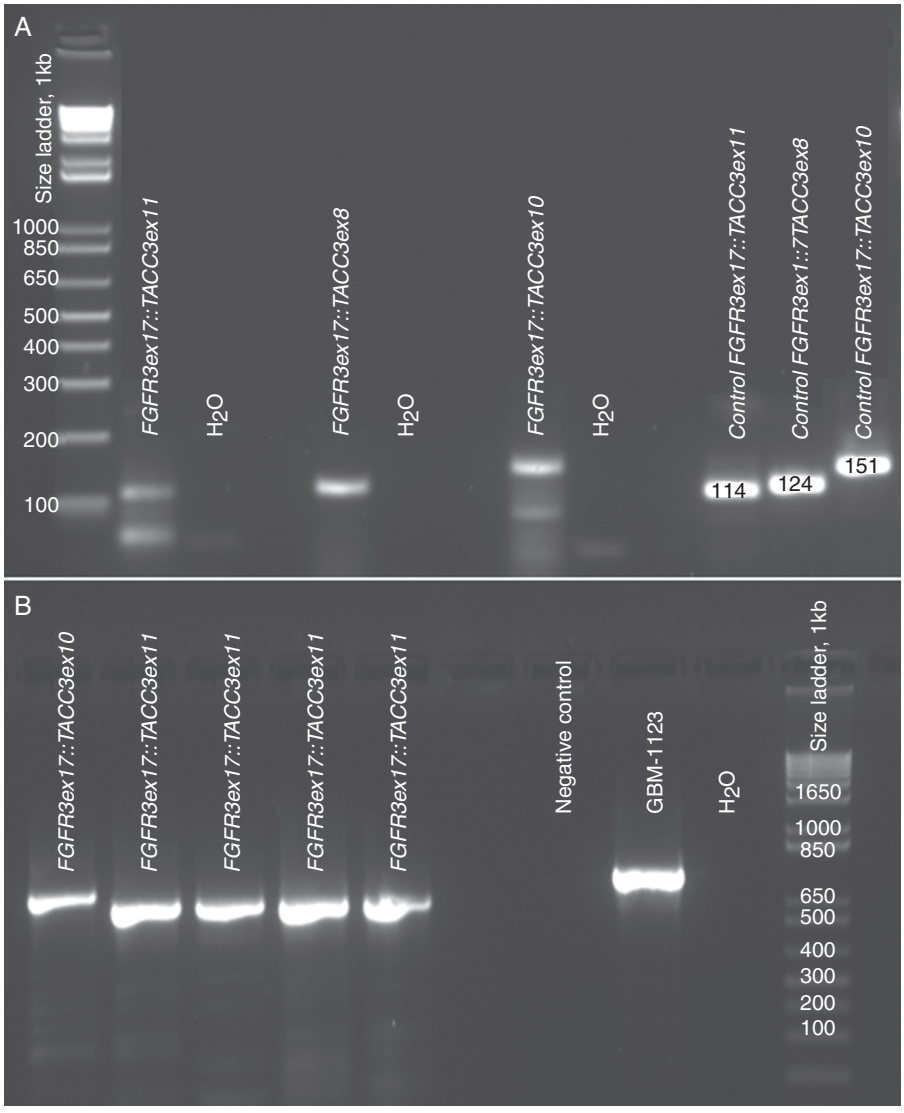

Figure 3. (A) RT-PCR results of FFPE material of 3 glioma samples, showing the 3 most frequently observed fusion variants as detected in Case 4, Case 10, and Case 2, respectively. Per control lane, the length (bp) that the product is expected to have is presented in the signal. Nonspecific products below 100 bp are considered to be primer-dimers. 1-kb DNA size ladder. (B) RT-PCR results of 5 fresh frozen GBM samples (Cases 2, 4, 5, 6, and 8) revealing *FGFR3::TACC3* fusions. FGFR3ex17TACC3ex11 means that exon 17 of FGFR3 gene is fused to exon 11 of TACC3 gene. Positive control: GBM-1123 cell line (Singh et al.[5]); negative control: sample with an EWS-FLI1 translocation. 1-kb DNA size ladder.

suppression of FGFR3 protein expression by miRNA-99A.[11] However, recently, 3 cases were described in which an *FGFR3::TACC3* fusion co-existed with an *FGFR3* K650T mutation.[28] The prognostic and predictive meaning of the *FGFR3* mutation and FGFR3 overexpression in this case without *FGFR3::TACC3* fusion remains unknown. Currently, this RT-PCR assay for FFPE material tests for 5 common fusion variants. It is still possible that the 2 samples with positive FGFR3 staining on IHC, but no fusion detected on RT-PCR (Case 1 and Case 11) do harbor an *FGFR3::TACC3* fusion as RNAseq was unsuccessful in these cases.

Because FF material is not always available in the diagnostic setting, it is helpful that RT-PCR can also be performed on FFPE material, using the same RT-PCR protocol and reagents, but different primers: 1 primer pair detecting large amplicons in the range of 1000 bp for FF, and 5 primer pairs detecting amplicons in the range between 100 and 200 bp for FFPE. The presence of nonspecific amplicons and the possibility of false negative results as a result of RNA degradation, warrant caution when performing RT-PCR on FFPE material. In our experience, RT-PCR was more challenging on older archival FFPE material, but will likely be easier on FFPE material during the initial diagnostic process as the tissue block is freshly prepared, making RNA fragmentation less severe. In an FFPE assay, it is essential to include controls to check for RNA fragmentation. It would be ideal to have a primer set covering all 15 previously described fusion variants of *FGFR3::TACC3*[18] for FPPE, so that in the absence of FF material, a complete diagnostic test for *FGFR3::TACC3* fusion can still be performed. The fact that in this study we only had

5 primer sets, allowing for the detection of 5 *FGFR3:TACC3* fusion variants, is a limitation of this study. By adding 2 additional sets of primers (*FGFR3*ex16-*TACC3*ex3 and *FGFR3*ex18*::TACC3*ex11) to the currently described assay, for which only 2 new primers would have to be designed, 77% of fusion variants could be detected. If available, FF is still preferred over FFPE because of the above-mentioned challenges when using FFPE and because of the high input required for successful RT-PCR when FFPE tissue is used.

It has been suggested to use a combined immune-reactivity score (IRS, staining intensity [range 0–3] × staining quantification (range 1–4 based on percentage of tumor cells that stain, at 25% intervals), with a cutoff value for overexpression set at an IRS of 7 or more.[29] In our experience, it is worth testing for *FGFR3* fusions in all cases with some staining upon FGFR3 IHC. Several of our cases with heterogeneous, low staining intensity did harbor an *FGFR3::TACC3* fusion, while these cases might not have reached the cutoff of IRS score 7 for FGFR3 expression. In this study, all cases with 2+ staining on IHC were confirmed to have an *FGFR3::TACC3* fusion, suggesting that additional testing for cases with clear expression of FGFR3 on IHC might not be necessary. However, since the numbers in this study are low, and positive staining for FGFR3 is rare, it might be worth testing all samples that show some positive staining.

In line with previously reported incidence, we found 9 samples with *FGFR3::TACC3* fusions in a cohort of 353 cases (2.5%; 2.9% of 308 cases with interpretable FGFR3 IHC), 8 of which we were able to detect using RT-PCR. The small sample size is another limitation of this study. For implementation of this technique in clinical practice, it would be desired to further validate the technique on a larger number of samples, for example, by temporarily running the RT-PCR assay alongside another detection method. Higher numbers of *FGFR3::TACC3* fusion-positive samples could be achieved if several labs combine their data. For the implementation of RT-PCR assay in routine clinical practice, we would advise to screen for FGFR3 overexpression using IHC, and to test samples with any overexpression in tumor cells. For the time being, testing for this aberration would be most clinically relevant for patients who have a chance to enter current or future clinical trials.

In conclusion, in the absence of FF material, RT-PCR to test for the presence of an *FGFR3::TACC3* fusion can still be performed on FFPE material, using the same protocol with different primer sets and a higher cDNA input. In this way, eligibility for treatment with an FGFR3 inhibitor can still be assessed, also when only a routinely processed tumor tissue sample is available.

Supplementary material

Supplementary material is available online at *Neuro-Oncology* (https://academic.oup.com/neuro-oncology).

Funding

No funding was acquired for this research.

Acknowledgments

We would like to thank Anne G.M. Hoskam for her contributions in setting up the RT-PCR for FFPE samples and for the laboratory work she performed and Aline N. de Paiva Paixao Becker, MD, PhD, for checking the IDH1 immunohistochemistry of the TMA samples.

Conflict of interest statement

The authors declare no conflict of interest.

Author contributions

J.v.K. and A.G.M.H. (acknowledgements) set up the RT-PCR for FFPE samples under supervision of W.E.J.d.L. P.A.R. selected and gathered the samples for the creation of the tissue microarray (TMA). W.v.H. scored FGFR3 IHC stainings on TMA and whole slide. J.v.K., A. G.M.H., and L.P.P.-A. performed the laboratory testing. L.P.P.-A. wrote the manuscript with input from all authors and created visual representations of the outcomes. All authors read and approved the manuscript.

Affiliations

Department of Pathology, University Medical Center Utrecht, Utrecht, The Netherlands (L.P.P.-A., J.v.K., W.v.H., W.W.J.d.L.); Princess Máxima Center for Pediatric Oncology, Utrecht, The Netherlands (B.B.J.T., P.W.); Department of Pathology, Amsterdam University Medical Centers/VUmc & Brain Tumor Center Amsterdam, Amsterdam, The Netherlands (P.W.); Department of Biochemistry and Molecular Biology, Sylvester Comprehensive Cancer Center, University of Miami, Miller School of Medicine, Miami, Florida, USA (A.L.); Department of Neurological Surgery, Sylvester Comprehensive Cancer Center, University of Miami, Miller School of Medicine, Miami, Florida, USA (A.I.); Department of Neurosurgery, University Medical Center Utrecht, Utrecht, The Netherlands (P.A.R.)

References

1. Ostrom QT, Gittleman H, Truitt G, et al. CBTRUS statistical report: primary brain and other central nervous system tumors diagnosed in the United States in 2011-2015. *Neuro Oncol*. 2018;20(suppl_4):iv1–iv86.
2. Di Stefano AL, Fucci A, Frattini V, et al. Detection, characterization, and inhibition of FGFR-TACC fusions in IDH wild-type glioma. *Clin Cancer Res*. 2015;21(14):3307–3317.
3. Zhang Y, Dong W, Zhu J, et al. Combination of EZH2 inhibitor and BET inhibitor for treatment of diffuse intrinsic pontine glioma. *Cell Biosci*. 2017;7(1):1–10.

4. Parker BC, Annala MJ, Cogdell DE, et al. The tumorigenic FGFR3-TACC3 gene fusion escapes miR-99a regulation in glioblastoma. *J Clin Invest*. 2013;123(2):855–865.
5. Singh D, Chan JM, Zoppoli P, et al. Transforming fusions of FGFR and TACC genes in human glioblastoma. *Science (New York, N.Y.)*. 2012;337(6099):1231–1235.
6. Mata DA, Benhamida JK, Lin AL, et al. Genetic and epigenetic landscape of IDH-wildtype glioblastomas with FGFR3-TACC3 fusions. *Acta Neuropathol Commun*. 2020;8(1):186.
7. Kleinschmidt-DeMasters BK, Gilani A. Extra-CNS and dural metastases in FGFR3::TACC3 fusion+ adult glioblastoma, IDH-wildtype. *Neurooncol Pract*. 2022;9(5):449–455.
8. Gilani A, Davies KD, Kleinschmidt-DeMasters BK. Can adult IDH-wildtype glioblastomas with FGFR3:TACC3 fusions be reliably predicted by histological features? *Clin Neuropathol*. 2021;40(3):165–167.
9. Di Stefano AL, Picca A, Saragoussi E, et al. Clinical, molecular, and radiomic profile of gliomas with FGFR3-TACC3 fusions. *Neuro Oncol*. 2020;22(11):1614–1624.
10. Brennan C. Neuro-oncology FGFR-TACC approaches the first turn in the race for targetable GBM mutations. *Neuro Oncol*. 2017;19(4):461–462.
11. Granberg KJ, Annala M, Lehtinen B, et al. Strong FGFR3 staining is a marker for FGFR3 fusions in diffuse gliomas. *Neuro Oncol*. 2017;19(9):1206–1216.
12. Lasorella A, Sanson M, Iavarone A. FGFR-TACC fusions in human glioma. *Neuro Oncol*. 2017;19(4):475–483.
13. Frattini V, Pagnotta SM, Tala W, et al. A metabolic function of FGFR3-TACC3 gene fusions in cancer. *Nature*. 2018;553(7687):222–227.
14. Costa R, Carneiro BA, Taxter T, et al. FGFR3-TACC3 fusion in solid tumors: mini review. *Oncotarget*. 2016;7(34):55924–55938.
15. Tabernero J, Bahleda R, Dienstmann R, et al. Phase I dose-escalation study of JNJ-42756493, an oral pan-fibroblast growth factor receptor inhibitor, in patients with advanced solid tumors. *J Clin Oncol*. 2015;33(30):3401–3408.
16. Wang Y, Liang D, Chen J, et al. Targeted therapy with anlotinib for a patient with an oncogenic FGFR3-TACC3 fusion and recurrent glioblastoma. *Oncologist*. 2020;26(3):5.
17. Gött H, Uhl E. FGFR3-TACCs3 fusions and their clinical relevance in human glioblastoma. *Int J Mol Sci*. 2022;23(15):8675.
18. Gallo LH, Nelson KN, Meyer AN, Donoghue DJ. Functions of fibroblast growth factor receptors in cancer defined by novel translocations and mutations. *Cytokine Growth Factor Rev*. 2015;26(4):425–449.
19. Bielle F, Di Stefano AL, Meyronet D, et al. Diffuse gliomas with FGFR3-TACC3 fusion have characteristic histopathological and molecular features. *Brain Pathol*. 2018;28(5):674–683.
20. McDonald MF, Athukuri P, Anand A, et al. Varied histomorphology and clinical outcomes of FGFR3-TACC3 fusion gliomas. *Neurosurg Focus*. 2022;53(6):E16.
21. Theelen WSME, Mittempergher L, Willems SM, et al. FGFR1, 2 and 3 protein overexpression and molecular aberrations of FGFR3 in early stage non-small cell lung cancer. *J Pathol Clin Res*. 2016;2(May):223–233.
22. Richardson SO, Huibers MMH, Weger RAD, et al. One-fits-all pretreatment protocol facilitating Fluorescence In Situ Hybridization on formalin-fixed paraffin- embedded, fresh frozen and cytological slides. *Mol Cytogenet*. 2019;12(27):1–10.
23. Schildhaus H, Heukamp LC, Merkelbach-bruse S, et al. Definition of a fluorescence in-situ hybridization score identifies high- and low-level FGFR1 amplification types in squamous cell lung cancer. *Mod Pathol*. 2012;25(11):1473–1480.
24. De Leng WWJ, Gadellaa-Van Hooijdonk CG, Barendregt-Smouter FAS, et al. Targeted next generation sequencing as a reliable diagnostic assay for the detection of somatic mutations in tumours using minimal DNA amounts from formalin fixed paraffin embedded material. *PLoS One*. 2016;11(2):e0149405.
25. Hehir-Kwa JY, Koudijs MJ, Verwiel ETP, et al. Improved gene fusion detection in childhood cancer diagnostics using RNA sequencing. *JCO Precis Oncol*. 2022;6:e200050–6.
26. Haas BJ, Dobin A, Li B, et al. Accuracy assessment of fusion transcript detection via read-mapping and de novo fusion transcript assembly-based methods. *Genome Biol*. 2019;20(1):1–16.
27. Helsten T, Elkin S, Arthur E, et al. The FGFR landscape in cancer: analysis of 4,853 tumors by next-generation sequencing. *Clin Cancer Res*. 2016;22(1):259–267.
28. Ballester LY, Moghadamtousi SZ, Leeds NE, et al. Coexisting FGFR3 p K650T mutation in two FGFR3-TACC3 fusion glioma cases. *Acta Neuropathol Commun*. 2019;7(63):1–4.
29. Schittenhelm J, Ziegler L, Sperveslage J, et al. FGFR3 overexpression is a useful detection tool for FGFR3 fusions and sequence variations in glioma. *Neurooncol Pract*. 2021;8(2):209–221.